Frequency Band Rejection Technique Based on the Operating Modes for a Wideband H-Shaped DRA

Feras Z. Abushakra and Nathan Jeong

Department of Electrical and Computer Engineering
University of Alabama, Tuscaloosa, 35487, USA
fabushakra@crimson.ua.edu, shjeong@eng.ua.edu

Abstract ─ In this paper, a new approach to create frequency band rejection is applied to a wideband H-shaped dielectric resonator antenna (DRA). In order to create a notch characteristic in the operating band of the $TE^{y}_{1\delta1}$ and $TE^{y}_{2\delta1}$ modes, and guided by their theoretical and simulated electric field distributions, a narrow conductive strip is incorporated around the mid-section of the H-shaped DRA. The orientation of the notching strip is determined based on the electric field distribution of the selected modes for the frequency rejection. Furthermore, the selected feeding method improves the radiation patterns for this DRA shape compared to its previous designs. The new design offers an operating frequency range that extends from 4.15 to 9.8 GHz, allowing 81% of fractional bandwidth. The first notch is created at 6.5 GHz, while the second one is at 8 GHz. Average radiation efficiency of 95% across the frequency of interest is achieved with overall dimensions of 40×30×11.4 mm^3. The proposed design is simulated using Ansys HFSS and validated by measurement.

Index Terms ─ Dielectric Resonator Antenna (DRA), H-shaped antenna, modes distribution, notch rejection.

I. INTRODUCTION

During the last few decades a great attention has been paid to the DRAs due to their capabilities to provide wide bandwidth, high gain, and high radiation efficiency compared to other types of antennas. Many shapes and feeding methods of DRAs were introduced for various applications such as 5G, WiMAX, radar, etc. [1]. Different feeding mechanisms to excite the DRA were also used such as microstrip transmission lines, coaxial probe and slot aperture [2]. The coaxial feeding method is the most commonly used method due to its matching flexibility by changing the probe position and height [3]. Various shapes of the DRA were presented (P, Z and T), where some of them were fed by microstrip line feeder, while others were fed by a probe [4-9]. In the last few years, many designs of the DRA showed that the single element DRA could achieve a bandwidth up to 120% [10-13]. This extremely wide band covers many applications where in some cases the interference becomes the main obstacle and needs to be suppressed. To overcome this problem, many designs suggested different methods to create notches in the operating band of wide band DRAs. In [10], an inverted conical shaped DRA fed directly by a circular ring patch antenna was presented. A notch rejection was created and shifted by changing the dimensions of the patch resonator. Also, several wide band DRA designs fed by a microstrip line feeder with notch characteristics were reported [11, 12]. For these designs, several modifications in the feeder or ground plane were done to create a stop band filtering in the operating bandwidth of the design. On the other hand, the DRA position was rotated with respect to the microstrip line feeder to create the notch characteristics [13]. In addition, a cross slot aperture was formed in a circular patch antenna placed directly underneath the DRA at the same side of the substrate. Two different etches in the microstrip patch antenna were conducted to create two frequency rejection bands [14]. These designs covered wide bandwidth up to 120%. Also, the DRA size is very small compared to the lower operating band in these designs. In such a hybrid method, the broadband response comes from both the microstrip feeder and DRA. Accordingly, such designs created the rejection band in the microstrip line feeder operating band while the DRA modes were not affected. On the other hand, UWB DRA was proposed with frequency rejection and fed using metallic strip with a probe on the side of the DRA with the presence of a shorting pin drilled inside the DRA [15]. A slot was created in the feeding vertical strip to create a notch in the operating band of the antenna. In this paper, a wide band H-shaped DRA with enhanced radiation pattern is presented. In order to create the notch frequency for the first two modes in the operating band, a narrow strip will be used to suppress part of the operating mode by wrapping it around the DRA in different directions. The antenna performance is discussed before and after applying the notching technique on this design.

Submitted On: August 22, 2020
Accepted On: December 6, 2020

https://doi.org/10.47037/2020.ACES.J.360208

II. ANTENNA DESIGN AND CONFIGURATION

The proposed H-shaped DRA is shown in Fig. 1. The excitation is realized with a U-shaped feeder which is directly connected to a coaxial probe. At the opposite side, another identical strip is placed and shorted to the ground. This feeding mechanism will be useful to create the $TE_{1\delta 1}$ and $TE_{2\delta 1}$ modes as the first two operating modes [16].

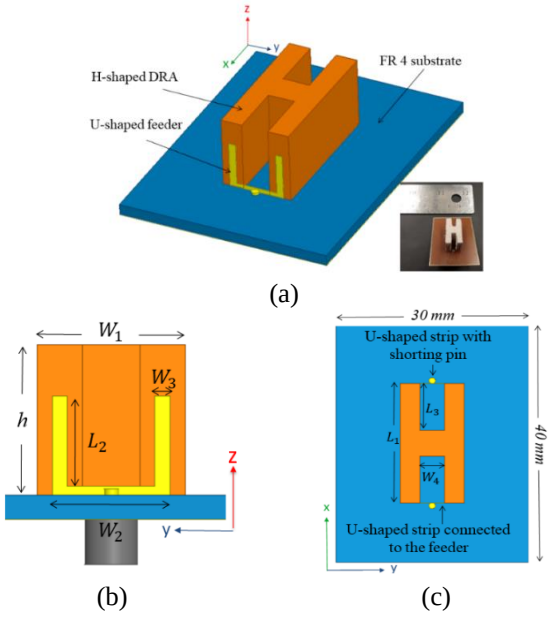

Fig. 1. The proposed H-shaped DRA: (a) 3D view with fabricated prototype, (b) *yz*-plane, and (c) *xy*-plane.

Among the different DRA shapes, the H-shape has the advantage of providing a symmetric geometry from the three principal axes. However, the radiation pattern of this shape has two problems. The cross polarization level is very high and the symmetry of the radiation pattern is poor at the perpendicular plane to the feeder. To address these issues, the proposed design is fed by two identical U-shaped strips. One for feeding the DRA while the other one is attached to the opposite side of the DRA and connected to the ground plane using via. This feeding method creates electric fields that allow the higher order modes to be more uniform and resulting in lower cross polarization level. In order for a better understanding of the second strip effects on the design, the electric field vector plots for the DRA with and without the second U-shaped strip are compared in Fig. 2. It could be seen that the electric field vectors at the mid-section show more uniform distribution in the DRA with the second U-strip at the 9 GHz. Also, the electric field shows better symmetry in its intensity at both sides of the design.

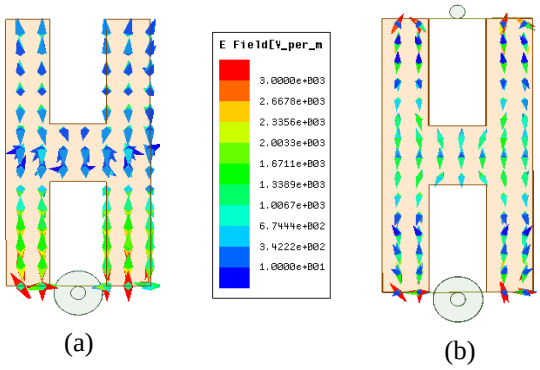

Fig. 2. Vector plot of the electric field at the *xy*-plane at 9 GHz. (a) DRA without the second U-shaped strip, and (b) DRA with the second U-shaped strip.

The DRA is placed directly at the top of 40×30×1.6 mm^3 FR-4 substrate with relative permittivity and dielectric loss tangent of (ϵ_r =4.4) and (tanδ=0.02), respectively. The ground plane is at the lower side of the substrate. For the DRA, Rogers RO 3010 material with a relative permittivity of 10.2 and dielectric loss tangent of 0.0035 is used. The design dimensions are W_1=10 mm, L_1=20 mm, L_3=7.85 mm, W_4=3.8 mm and h=11.4 mm. The feeder dimensions are L_2=6 mm, W_2=7.9 mm, and W_3=1 mm. The simulated and measured results of the design are shown in Fig. 3. The -10 dB impedance bandwidth is achieved from 4.85 to 9.8 GHz, 69% of the fractional bandwidth. The simulated peak realized gain is between 4.0 to 7.0 dBi. The measurement shows good agreement with the simulation. However, the slight difference between the measured and simulated performance is expected as there are many different substrate layers glued to fabricate the design.

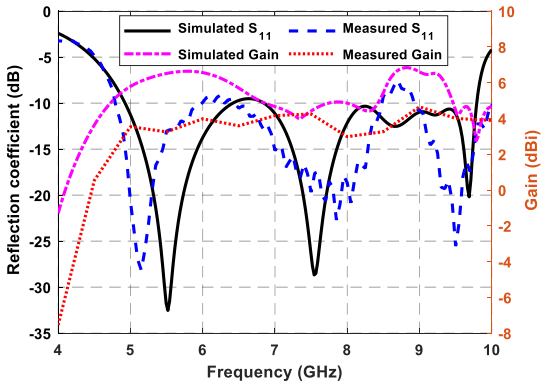

Fig. 3. Reflection coefficient and peak realized gain of the H-shaped DRA.

The radiation patterns of this design are illustrated in Fig. 4. The cross-polarization level is around -20 dB at the *yz*-plane, while it is less than -50 dB at the *xz*-plane

which is not shown in the scale. It is also notable that even at the end of the band, the cross polarization level remains low. The radiation pattern at the *yz*-plane shows highly symmetric pattern, while it is less symmetric at the *xz*-plane. However, compared to the previously reported H-shaped DRA, this design has better radiation patterns in terms of cross polarization level and symmetry [17, 18]. The front to back ratio (F/B) is around 10 dB.

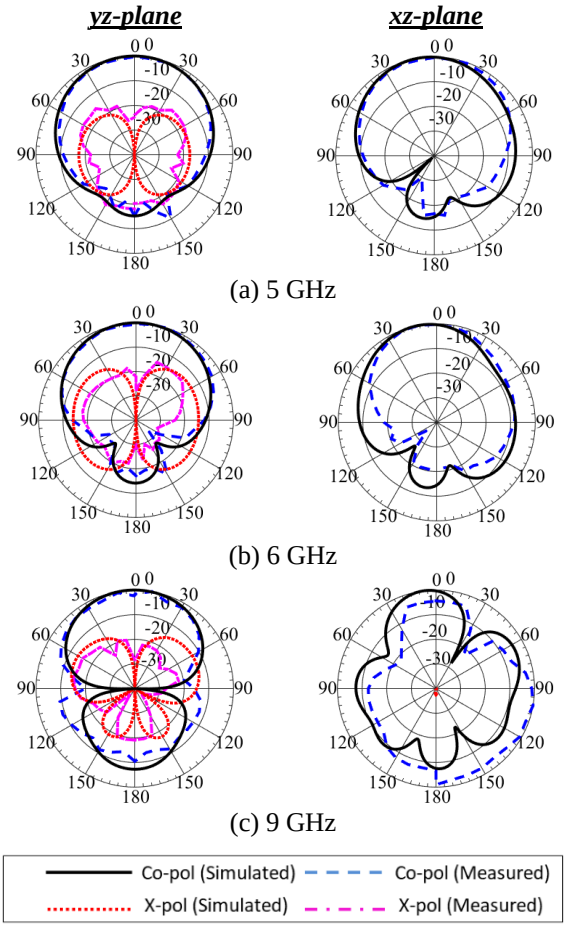

Fig.4. Radiation patterns of the H-shaped DRA at different frequencies.

For the operating modes in the DRA design, it could be seen at Fig. 3 that the first resonance is at 5.5 GHz, which is corresponds to the DRA dominant $TE_{1\delta1}$ mode. This mode has a uniform electric field distribution through the DRA geometry. For the second resonance at 7.6 GHz, it appears that the $TE_{2\delta1}$ mode starts to propagate [19]. The $TE_{2\delta1}$ mode has sinusoidal shape for the electric field vectors with a minimum electric field at the center of the DRA. This mode exists in this design as the DRA is placed on the substrate directly, while it will not propagate if it is placed on the ground plane [20]. The simulated electric field vector for the first and second resonances are plotted at the *xz*-plane in Fig. 5. It could be seen that the electric field distributions align well with the theory of these modes.

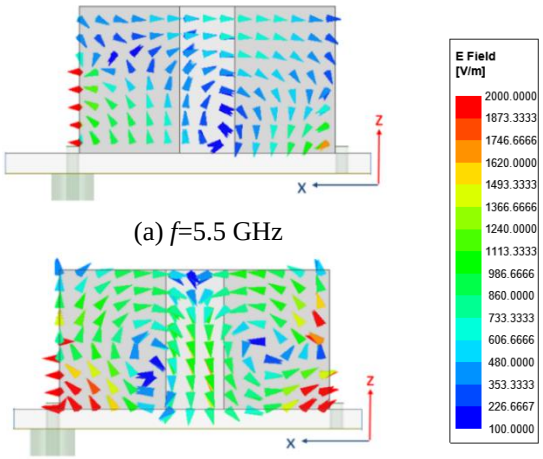

Fig. 5. Electric field vectors plot at the *xz*-plane at different frequencies.

III. FREQUENCY BAND REJECTION

In this section, a new method to create frequency rejection band for the first two operating modes for the DRA in general will be presented. Unlike previous literature where several modifications in the microstrip line feeder were made to create a stop band filtering in the bandwidth of the design, this design will create the frequency rejection in the operating modes of the DRA using open-circuited conductive strips. As shown in Fig. 6 (a), the $TE_{1\delta1}$ mode has uniform distribution across the *xz*-plane. This mode extends from the beginning of the operating band reaching just before the second mode that starts to propagate slightly before 7.6 GHz. In order to create the notch effectively in its operating band, it is essential to look at the electric field intensity of the DRA near the frequency where the notch needs to be created. It could be clearly seen that the electric field is minimum at the mid-section parallel to the x-axis. Therefore, a narrow conductive strip with 1 mm width is employed in parallel to the long sides of the H-shaped DRA to create the notch at the middle of the dominant mode. The strip is wrapped around the DRA and reaches to the substrate, as shown in Fig. 6 (b). The VSWR for this design is plotted in Fig. 7. Through the band from 4.5 to 9.8 GHz, the VSWR value is under 2 except at the middle of the operating band of the first mode, where the VSWR value increases. The center of the rejection band is controlled by adjusting the value of the DRA height (*h*). As expected, larger size of the DRA, (i.e., higher *h*), will shift the notch center to the lower frequency band [21].

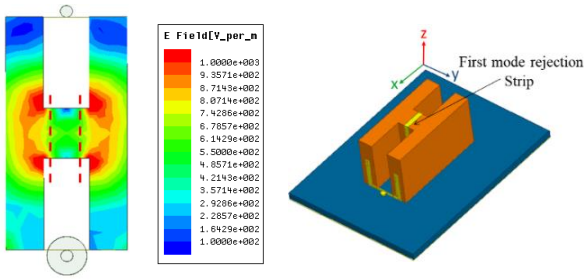

(a) (b)

Fig. 6. Notch rejection at the first mode at 6.5 GHz: (a) electric field magnitude at *xy*-plane, and (b) conducting strip applied at the mid-section of the DRA.

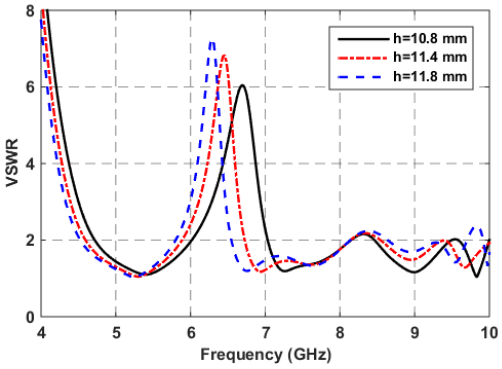

Fig. 7. VSWR curves for the first notch design with different values of (*h*).

On the other hand, for the $TE_{2\delta 1}$ mode, the electric field magnitude has a null at the mid-section parallel to the y-axis as shown in Fig. 8 (a). This region where the electric field vectors of the two sinusoidal waves are cancelling each other in Fig. 5 (b). To create the notch within this mode a conductive strip parallel to the y-axis is wrapped on the DRA, as shown in Fig. 8(b).

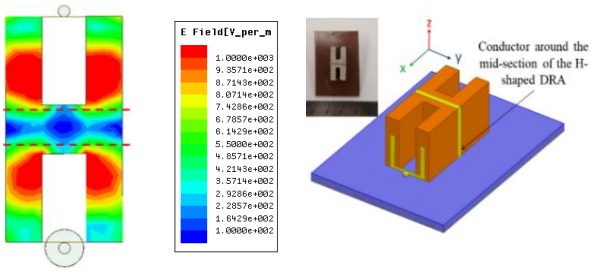

(a) (b)

Fig. 8. Notch rejection at the second mode at 8 GHz: (a) electric field magnitude at *xy*-plane, and (b) conducting strip for the second notch rejection with fabrication.

Figure 9 shows the VSWR for the band rejection for the $TE_{2\delta 1}$ mode with different values of (*h*). The overall operating band extends from 4.15 to 9.8 GHz, achieving 81% fractional bandwidth. The comparison between the simulated and measured VSWR at *h*=10.8 mm is plotted in Fig. 10 where they are in good agreement with slight frequency shift which may be caused by the fabrication tolerance. At 8 GHz, where the stop band occurs, the peak gain falls to less than -6 dBi and the radiation efficiency is less than 30%, while achieving around 95% through the band of interest as shown in Fig. 11.

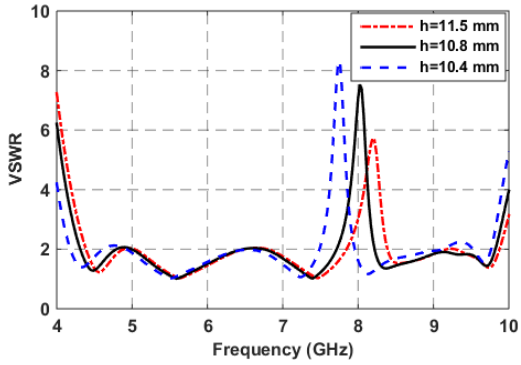

Fig. 9. VSWR curves for the second notch with different values of (*h*).

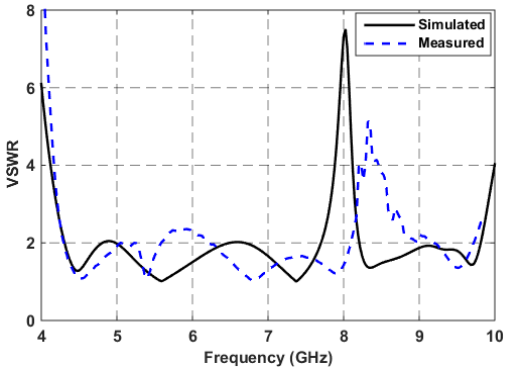

Fig. 10. Measured VSWR for the second notch design (*h*=10.8 mm).

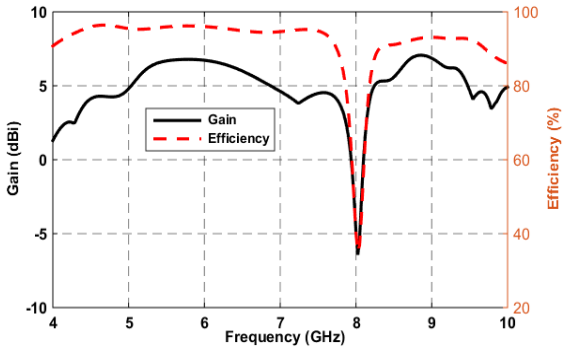

Fig. 11. Peak gain and efficiency for the second notch design (*h*=10.8 mm).

To investigate the effects of adding the notching strip on the radiation patterns of the design, the radiation patterns after adding the strip is plotted as shown in Fig. 12. It could be seen that the radiation patterns are still almost the same with the strip.

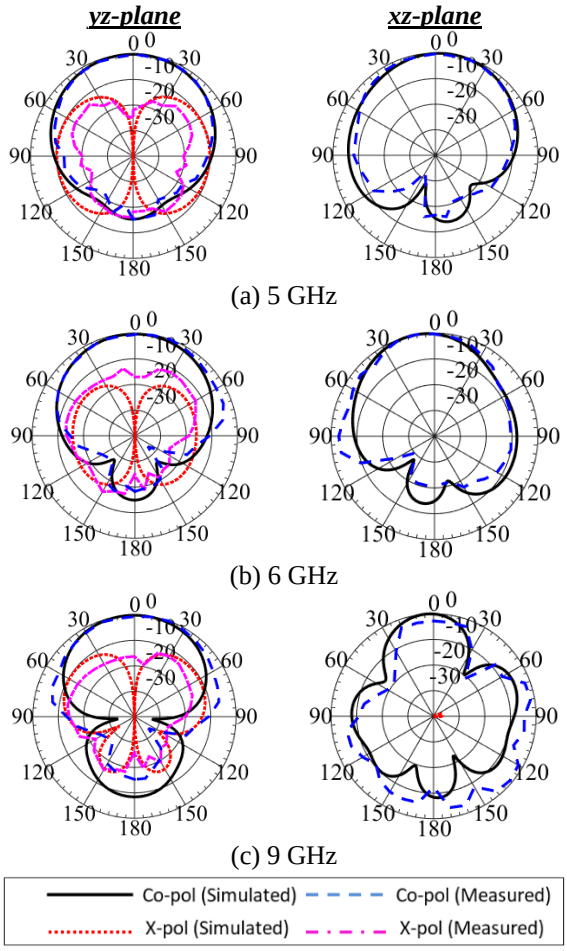

Fig. 12. Radiation patterns of the H-shaped DRA with the second notch rejection at 8 GHz (h=10.8 mm).

IV. CONCLUSIONS

A new method to create frequency band rejection was proposed in this paper. The new method depends on the electric field distribution of the operating modes to create the notch using a strip around the DRA. The first notch was created at the $TE^{y}_{1\delta1}$ mode band while the second notch was created within the $TE^{y}_{2\delta1}$ mode frequency region. The design covers a wideband up to 81% of fractional bandwidth, with 95% radiation efficiency and stable gain throughout the operating band. Furthermore, the radiation patterns of this design showed better characteristics compared to the previous literature for the same shape. The presence of the strip has minimal effect on the radiation patterns of the design.

REFERENCES

[1] D. Soren, R. Ghatak, R. K. Mishra, and D. R. Poddar, "Dielectric resonator antennas: Designs and advances," *Progress in Electromagnetics Research B*, vol. 60, pp. 195-213, 2014.

[2] F. Z. Abushakra, A. S. Al-Zoubi, and D. F. Hawatmeh, "Design and measurements of rectangular dielectric resonator antenna linear arrays," *Applied Computational Electromagnetics Society Journal (ACES)*, vol. 33, no. 4, pp. 380-387, 2018.

[3] I. A. Eshrah, A. A. Kishk, A. B. Yakovlev, and A. W. Glisson, "Excitation of dielectric resonator antennas by a waveguide probe: Modeling technique and wide-band design," *IEEE Trans. on Antennas and Propagation*, vol. 53, no. 3, pp. 1028-1037, 2005.

[4] M. Khalily, M. K. A. Rahim, A. A. Kishk, and S. Danesh, "Wideband P-shaped dielectric resonator antenna," *Radioengineering*, vol. 22, no. 1, 2013.

[5] A. Sharma and R. K. Gangwar, "Circularly polarised hybrid Z-shaped cylindrical dielectric resonator antenna for multiband applications," *IET Microwaves, Antennas & Propagation*, vol. 10, no. 12, pp. 1259-1267, 2016.

[6] R. Cicchetti, A. Faraone, E. Miozzi, R. Ravanelli, and O. Testa, "A high-gain mushroom-shaped dielectric resonator antenna for wideband wireless applications," *IEEE Trans. on Antennas and Propagation*, vol. 64, no. 7, pp. 2848-2861, 2016.

[7] J. Kumar, B. Mukherjee, and N. Gupta, "A novel tetraskelion dielectric resonator antenna for wideband applications," *Microwave and Optical Technology Letters*, Wiley, vol. 57, no. 12, pp. 2781-2786, 2015.

[8] F. Z. Abushakra, A. S. Al-Zoubi, I. Uluer, and D. F. Hawatmeh, "Ultra-wideband E-shaped dielectric resonator antennas fed by coaxial probe and trapezoidal conductor," *International Journal of Electronics Letters-Taylor and Francis*, pp. 1-10, doi: 10.1080/21681724.2020.1726475, 2020.

[9] F. Abushakra and A. Al-Zoubi, "Wideband vertical T-shaped dielectric resonator antennas fed by coaxial probe," *Jordan Journal of Electrical Engineering (JJEE)*, vol. 3, no. 4, pp. 250-258, 2017.

[10] M. Niroo-Jazi and T. A. Denidni, "Experimental investigations of a novel ultrawideband dielectric resonator antenna with rejection band using hybrid techniques," *IEEE Antennas and Wireless Propagation Letters*, vol. 11, pp. 492-495, 2012.

[11] M. Abedian, S. K. A. Rahim, S. Danesh, M. Khalily, and S. M. Noghabaei, "Ultrawideband dielectric resonator antenna with WLAN band rejection at 5.8 GHz," *IEEE Antennas and Wireless Propagation Letters*, vol. 12, pp. 1523-1526, 2013.

[12] M. Abedian, S. K. A. Rahim, S. Danesh, S. Hakimi, L. Y. Cheong, and M. H. Jamaluddin, "Novel design of compact UWB dielectric resonator antenna with dual-band-rejection characteristics for WiMAX/ WLAN bands," *IEEE Antennas and Wireless Propagation Letters*, vol. 14, pp. 245-248, 2015.
[13] M. Y. A. Shahine, M. Al-Husseini, K. Y. Kabalan, and A. El-Hajj, "Dielectric resonator antennas with band rejection and frequency configurability," *Progress in Electromagnetics Research C*, vol. 46, pp. 101-108, 2014.
[14] U. A. Dash and S. Sahu, "UWB dual-band notched conical dielectric resonator antenna with improved gain," *IETE Journal of Research-Taylor and Francis*, 2018.
[15] Y. F. Wang, T. A. Denidni, Q. S. Zeng, and G. Wei, "Band-notched UWB rectangular dielectric resonator antenna," *Electronics Letters*, vol. 50, no. 7, pp. 483-484, 2014.
[16] A. Guptaa and R. K. Gangwar, "New excitation scheme to excite higher-order radiating modes in rectangular dielectric resonator antenna for microwave applications," *Journal of Microwave Power and Electromagnetic Energy*, vol. 52, no. 3, pp. 240-251, 2018.
[17] X. Liang and T. A. Denidni, "H-shaped dielectric resonator antenna for wideband applications," *IEEE Antennas and Wireless Propagation Letters*, vol. 7, pp. 163-166, 2008.
[18] N. A. Jaafar, M. H. Jamaluddin, J. Nasir, and N. M. Noor, "H-shaped dielectric resonator antenna for future 5G application," *2015 IEEE International RF and Microwave Conference (RFM)*, pp. 115-117, 2015.
[19] R. S. Yaduvanshi and H. Parthasarathy, *Rectangular Dielectric Resonator Antennas*. Springer India, 2016.
[20] A. Petosa, *Dielectric Resonator Antenna Handbook*. Artech House Publishers, 2007.
[21] A. A. Kishk and W. Huang, "Size-reduction method for dielectric-resonator antennas," *IEEE Antennas and Propagation Magazine*, vol. 53, no. 2, pp. 26-38, 2011.

Feras Abushakra received his B.Sc. degree in Electrical Engineering majoring in Communications and Electronics from the Jordan University of Science and Technology (JUST), Irbid, Jordan. He obtained his M.Sc. degree in Wireless Communication Engineering from Yarmouk University, Jordan, in 2017. He is currently working towards his Ph.D. in Electrical Engineering at the University of Alabama (UA), Tuscaloosa. His researches focus on dielectric resonator antennas, patch antennas, arrays and radar systems.

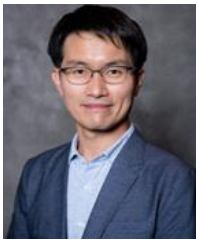

Nathan Jeong received his Ph.D. degree in Electrical and Computer Engineering from Purdue University, 2010. At 2018 he joined the University of Alabama as Assistant Professor. His current research interests include 5G millimeter-wave antenna and system, adaptive RF front-ends and electromagnetics. He has total of 12 years of industrial experience at Samsung Electronics, BlackBerry and Qualcomm. In addition, he holds more than 60 international patent and patent applications in the areas of wireless communication circuit, microwave and millimeter wave system, V2X (Vehicle to Everything), antennas, wireless power transfer and bioelectronics.